

## Photon statistics and the optical Stark effect

T. Altevogt, H. Puff, and R. Zimmermann

*Max-Planck-Arbeitsgruppe Halbleitertheorie an der Humboldt-Universität zu Berlin, Hausvogteiplatz 5-7, D-10117 Berlin, Germany*

(Received 12 November 1996)

We theoretically describe a pump-probe scheme for detecting the optical Stark effect on two-level atoms with a fully quantized pump field. The probe absorption reflects the photon statistics of the pump field for both the single-atom and multiatom case. Nonclassical features, without counterpart in the single-atom case appear in the multiatom absorption and result in strong variations of the absorption amplitude and nonclassical gain or absorption. [S1050-2947(97)05708-9]

PACS number(s): 42.50.Ct, 42.50.Ar, 42.50.Hz

### I. INTRODUCTION

An extensively investigated phenomenon in modern spectroscopy is the optical (or dynamical) Stark effect. It is due to the dynamic coupling of atomic states by a quasiresonant electromagnetic field leading to shifts of the energy levels with respect to their original positions. After its first demonstration by Autler and Townes [1], the optical Stark effect has been investigated in a large variety of systems, for example, atomic and molecular systems [2,3] or excitons in semiconductors [4,5]. Theoretical descriptions of these experiments have usually relied on treating the electromagnetic field classically [6,7]. One feature neglected in this semiclassical approach is the dependence of the energy shift on the photon number as exemplified by the Jaynes-Cummings model [8,9]. For strong atom-field coupling, the shifted resonances are expected to reflect the photon statistics of the incident electromagnetic field, as has been proposed earlier for interband transitions in semiconductors [10]. Closely related are investigations of resonance fluorescence spectra dependent on field fluctuations [11–13].

Due to progress in highly sophisticated experimental techniques, nonclassical features of the radiation field have already been observed [14]. These results stimulate the investigation of effects in spectroscopic experiments that are due to the quantized radiation field.

The purpose of the present paper is to discuss the influence of photon statistics on Stark-shifted resonances detected in pump-probe experiments. It will be shown that the calculated absorption spectra of the probe field directly display the photon statistics of the pump field. The corresponding spectra for the multiatom case reveal a complex substructure which has no counterpart in the single-atom case and which results in a probe absorption highly sensitive to slight frequency changes. Another nonclassical feature is the appearance of probe gain (absorption) at frequencies where the semiclassical approach predicts absorption (gain).

In semiconductor physics, high-resolution pump-probe techniques are used to detect the optical Stark shift of excitonic resonances [15,16]. For narrow exciton lines, the photon statistics of the pump field could have an observable influence on the shape of the shifted probe absorption. In spite of this, the line broadening of an excitonic resonance would not allow the resolution of the complex substructures. In order to detect the latter, an extremely narrow absorption

line of a microwave, a near-infrared or a dipole-forbidden optical transition in an atom should be taken into consideration. Although their optical Stark shift has not been detected yet to our knowledge, ultranarrow atomic absorption lines have already been recorded in the microwave and the optical regime (e.g., [17–19]) by applying a detection scheme which is discussed by Cook and Kimble in [20].

The paper is organized as follows: In Sec. II, the Tavis-Cummings scheme [21] will be introduced and used to derive an expression for the probe absorption. In Sec. III, absorption spectra for the single-atom and multiatom case are presented and interpreted in terms of dressed states.

### II. THEORETICAL MODEL

#### A. Hamiltonian

The model system considered here consists of  $N_0$  identical two-level atoms with ground state  $|g\rangle$  and excited state  $|e\rangle$  confined in a high- $Q$  cavity. Their spatial localization is assumed to be in the Lamb-Dicke regime, i.e., the localization uncertainty is much less than the wavelength of both the pump and the probe field. The cavity is tuned to resonance with the pump mode, and the mean Rabi frequency  $\langle\Omega\rangle = 2g\sqrt{\langle n\rangle}$  (with  $g$  the atom-field coupling constant and  $\langle n\rangle$  the mean photon number) is assumed to be sufficiently high to neglect dissipative processes. Within these limits, the atom-field dynamics may be adequately described in the rotating-wave approximation by the Hamiltonian

$$H_0 = \sum_{\nu=1}^{N_0} \{ \hbar\omega_g g_{\nu}^{\dagger} g_{\nu} + \hbar\omega_e e_{\nu}^{\dagger} e_{\nu} \} + \hbar\omega_p \{ a^{\dagger} a + \frac{1}{2} \} + \hbar g \sum_{\nu=1}^{N_0} \{ g_{\nu}^{\dagger} e_{\nu} a^{\dagger} + a e_{\nu}^{\dagger} g_{\nu} \}, \quad (2.1)$$

where  $a$  and  $a^{\dagger}$  are annihilation and creation operators for a photon of the pump field and  $g_{\nu}(g_{\nu}^{\dagger})$ ,  $e_{\nu}(e_{\nu}^{\dagger})$  are the annihilation (creation) operators for an electron in the states  $|g\rangle$ ,  $|e\rangle$  of the  $\nu$ th atom. This Hamiltonian obviously conserves the number  $N_{\nu} = e_{\nu}^{\dagger} e_{\nu} + g_{\nu}^{\dagger} g_{\nu}$  of electrons at the  $\nu$ th atom, and the following considerations can be restricted to the subspace  $N_{\nu} = 1$ . With the collective atomic operators [22]

$$J_{+} = \sum_{\nu} e_{\nu}^{\dagger} g_{\nu}, \quad J_{-} = \sum_{\nu} g_{\nu}^{\dagger} e_{\nu},$$

$$J_3 = \frac{1}{2} \sum_{\nu} \{e_{\nu}^{\dagger} e_{\nu} - g_{\nu}^{\dagger} g_{\nu}\}, \quad (2.2)$$

the Hamiltonian can be rewritten as

$$H_0 = \hbar \delta J_3 + \hbar g \{J_+ a + a^{\dagger} J_-\} + \hbar \omega_p \left\{ a^{\dagger} a + J_3 + \frac{N_0}{2} \right\}, \quad (2.3)$$

where  $\delta = (\omega_e - \omega_g) - \omega_p$  denotes the pump detuning, and an irrelevant constant has been dropped.

The operators (2.2) obey the commutator relations  $[J_3, J_{\pm}] = \pm J_{\pm}$ ,  $[J_+, J_-] = 2J_3$  of a generalized angular momentum operator; its square  $J^2$  is constant in time. Another constant of motion is provided by the operator

$$\mathcal{K} = a^{\dagger} a + J_3 + \frac{N_0}{2}, \quad (2.4)$$

whose integer eigenvalues, the excitation numbers, count photons and excited atoms. The relevant dynamics of the coupled atom-photon system is governed by the reduced Hamiltonian

$$\mathcal{H}_0 = \hbar \delta J_3 + \hbar g \{J_+ a + a^{\dagger} J_-\}. \quad (2.5)$$

A simultaneous eigenstate  $|\mu, j, k\rangle$  of  $\mathcal{H}_0$ ,  $J^2$ , and  $\mathcal{K}$ ,

$$\mathcal{H}_0 |\mu, j, k\rangle = E_{\mu}(j, k) |\mu, j, k\rangle,$$

$$J^2 |\mu, j, k\rangle = j(j+1) |\mu, j, k\rangle, \quad \mathcal{K} |\mu, j, k\rangle = k |\mu, j, k\rangle, \quad (2.6)$$

is called the ‘‘dressed state,’’ and may be obtained from the uncoupled atom-photon basis  $\{|n; j, m\rangle\}$ , defined by

$$\begin{aligned} a^{\dagger} a |n; j, m\rangle &= n |n; j, m\rangle, \\ J^2 |n; j, m\rangle &= j(j+1) |n; j, m\rangle, \\ J_3 |n; j, m\rangle &= m |n; j, m\rangle, \\ n &= 0, 1, 2, \dots, \quad j = 0, 1, \dots, N_0/2, \\ m &= -j, -j+1, \dots, j, \end{aligned} \quad (2.7)$$

(provided  $N_0$  is even). A dressed state corresponding to a fixed excitation number  $k$  is a superposition of a finite number of uncoupled states, i.e., those obeying  $k = n + m + N_0/2$ .

### B. Absorption of the probe field

The quantity to be investigated is the absorption of a weak and monochromatic probe field of frequency  $\omega$ , which can be treated as a classical field [23]. This external field is, in the rotating-wave approximation, coupled to the system according to

$$H = H_0 + V, \quad V = \hbar \tilde{g} (J_+ \alpha e^{-i\omega t} + \text{H.c.}), \quad (2.8)$$

where the  $c$  number  $\alpha$  denotes the amplitude of the probe field. The coupling constant  $\tilde{g}$  is assumed to be much less

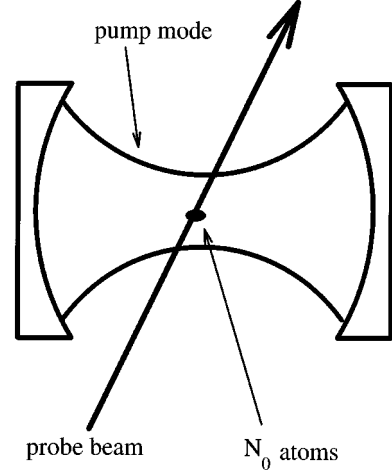


FIG. 1. Schematic pump-probe setup with the probe field being nonresonant to a cavity mode.

than  $g$ , as the test field is nonresonant to a cavity mode, as shown schematically in Fig. 1.

The detection of the time-integrated probe absorption is appropriately described by the response  $\chi(\omega)$  linear in  $\alpha$  which can be obtained by applying the Kubo formula [24] as

$$\begin{aligned} \chi(\omega) &= -i \hbar \tilde{g}^2 \lim_{T \rightarrow \infty} \frac{1}{T} \int_0^T dt \int_{-\infty}^t dt' \langle [J_-(t), J_+(t')] \rangle \\ &\quad \times e^{i(\omega - \omega_p)(t-t')}. \end{aligned} \quad (2.9)$$

The time-dependent operators are Heisenberg operators with respect to the reduced Hamiltonian  $\mathcal{H}_0$  of Eq. (2.5).

The angular brackets denote the expectation value with respect to the initial state. In the present case, atoms and photons are assumed to be initially decoupled, and all the atoms are in their ground states. Since  $J^2$  is conserved, only states with  $j = N_0/2$  are involved in the dynamics of the system, and the atomic states will be denoted by  $|m\rangle$  instead of  $|j = N_0/2, m\rangle$  in the following. The corresponding statistical operator for the initial state is therefore

$$\rho = \rho_{\text{pump}} \otimes |m = -N_0/2\rangle \langle m = -N_0/2|. \quad (2.10)$$

The linear susceptibility  $\chi(\omega)$  derived from Eq. (2.9) obeys the dispersion relation

$$\chi(\omega) = \lim_{\epsilon \rightarrow 0} \int_{-\infty}^{\infty} \frac{d\omega'}{\pi} \chi_2(\omega') \frac{1}{\omega - \omega' + i\epsilon}, \quad (2.11)$$

with

$$\chi_2(\omega) = \pi \hbar \tilde{g}^2 \sum_{\mu, \mu'} \sum_{n=0}^{\infty} g(\omega) \delta(\omega - \omega_p - \omega_{\mu, \mu'}(n)), \quad (2.12)$$

where  $g(\omega)$  is defined as

$$\begin{aligned} g(\omega = \omega_p + \omega_{\mu, \mu'}(n)) &= |\langle \mu', k' = n+1 | J_+ | \mu, k = n \rangle|^2 \\ &\quad \times \{ p_n |\langle \mu, k = n | n; m = -N_0/2 \rangle|^2 \\ &\quad - p_{n+1} |\langle \mu', k' = n+1 | n+1; m = -N_0/2 \rangle|^2 \}, \end{aligned} \quad (2.13)$$

and where the abbreviation  $\hbar\omega_{\mu,\mu'}(n) = E_{\mu'}(k'=n+1) - E_{\mu}(k=n)$  and the selection rule  $\langle \mu', k' | J_+ | \mu, k \rangle \propto \delta_{k', k+1}$  have been used. Due to the special initial state (2.10), the susceptibility depends only on the diagonal elements  $p_n = \langle n | \rho_{\text{pump}} | n \rangle$  of the statistical operator of the pump field, i.e., the photon-number distribution. The nondiagonal elements of  $\rho_{\text{pump}}$  do not appear in the linear response. The quantities  $|\langle \mu, k=n | n; m \rangle|^2$  determine the relative contribution of the bare state  $|n; m\rangle$  to the dressed state  $|\mu, k=n\rangle$ , i.e., its occupation probability. Their difference for two consecutive excitation numbers essentially fixes the sign of the weight  $g(\omega)$  at the corresponding transition frequency and thus discriminates between regions of absorption and gain.

### C. Semiclassical probe absorption

A semiclassical approach for the pump field, i.e., substituting the operators  $a$  and  $a^\dagger$  by the  $c$  numbers  $\sqrt{\langle n \rangle} e^{i\omega t}$  and  $\sqrt{\langle n \rangle} e^{-i\omega t}$ , leads to a much simpler expression for the linear response, i.e.,

$$\chi_2(\omega) \propto \left(1 + \frac{\delta}{\tilde{\Omega}}\right)^2 \delta(\omega - \omega_p - \tilde{\Omega}) - \left(1 - \frac{\delta}{\tilde{\Omega}}\right)^2 \delta(\omega - \omega_p + \tilde{\Omega}), \quad (2.14)$$

where  $\tilde{\Omega}$  denotes the generalized Rabi frequency given by

$$\tilde{\Omega} = \sqrt{4g^2 \langle n \rangle + \delta^2}. \quad (2.15)$$

Thus the semiclassical probe absorption consists of only two sharp resonance lines at frequencies  $\omega_{\pm} = \omega_p \pm \tilde{\Omega}$ , with a probe absorption at  $\omega_+$  and a probe gain at  $\omega_-$ .

## III. CALCULATED ABSORPTION SPECTRA AND INTERPRETATION

### A. Absorption for a single atom

In the single-atom case (Jaynes-Cummings model), the subsets of bare states mixed by  $H_0$  are

$$\{|n; m=1/2\rangle, |n+1; m=-1/2\rangle\}. \quad (3.1)$$

Without atom-photon coupling, these two states are separated energetically by the pump detuning  $\delta$ , as shown on the left-hand side of Fig. 2. The dressed states, shown on the right-hand side, are shifted relative to the bare states by the Stark shift

$$\Delta_n = \pm \frac{1}{2} \{ \sqrt{4g^2 n + \delta^2} - |\delta| \}. \quad (3.2)$$

Due to its dependence on the photon number  $n$ , it is different for each pair of dressed states with a common excitation number.

The photon statistics considered here are the well-known result of the simplified laser model [25]

$$p_n = \frac{(r\beta)^n}{(\beta+n)!} p_0, \quad (3.3)$$

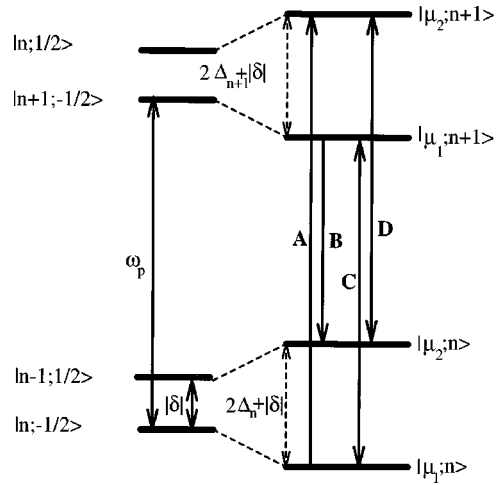


FIG. 2. Bare states and dressed states for the single-atom case.

where  $r$  indicates the pump parameter, i.e., the pump rate relative to the laser threshold, and  $\beta$  is a parameter depending on the decay rates of the upper and lower laser level.

In Fig. 3, the photon statistics for three choices of pump parameters  $r$  are shown, i.e., a thermal-like statistics for pumping below the laser threshold (triangles), slightly above the threshold (squares), and a Poisson-like shape for pumping considerably above threshold. In Fig. 4, the corresponding absorption spectra are shown where  $g(\omega)$  given by Eq. (2.13) indicates the positions and the heights of the absorption peaks. Four different groups of resonances are clearly recognized, denoted by  $A$ ,  $B$ ,  $C$ , and  $D$ . They are traced back to the corresponding transitions sketched in Fig. 2 and labeled accordingly. Since the pump detuning  $\delta$  is chosen in the range of the mean Rabi frequency  $\langle \Omega \rangle$ , the bare state  $|n; m=-1/2\rangle$  assigned to the atomic ground state dominates in the dressed state  $|\mu_1, k=n\rangle$ , whereas the state  $|n-1; m=1/2\rangle$  assigned to the excited atomic state dominates in  $|\mu_2, k=n\rangle$ . As the atom is initially in its ground state, transition  $A$  leads to an absorption, while transition  $B$  gives rise to a probe gain. Apart from spreading into groups of lines,  $A$  and  $B$  are found in the semiclassical treatment, too. Transitions  $C$  and  $D$  lead to resonances with small am-

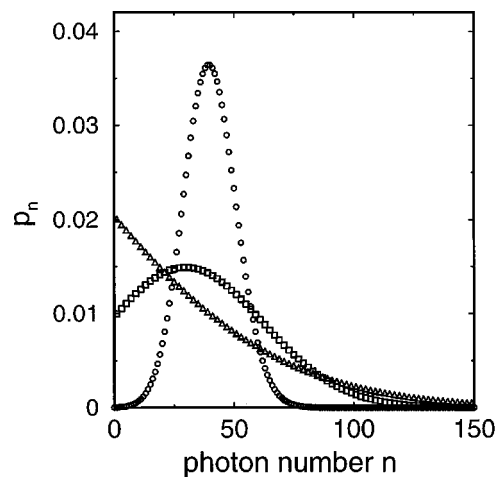


FIG. 3. Photon statistics of a laser for different pump parameters  $r$ : triangles,  $r=0.98$ ; squares,  $r=1.03$ ; circles,  $r=1.5$ ;  $\langle n \rangle = 40$ .

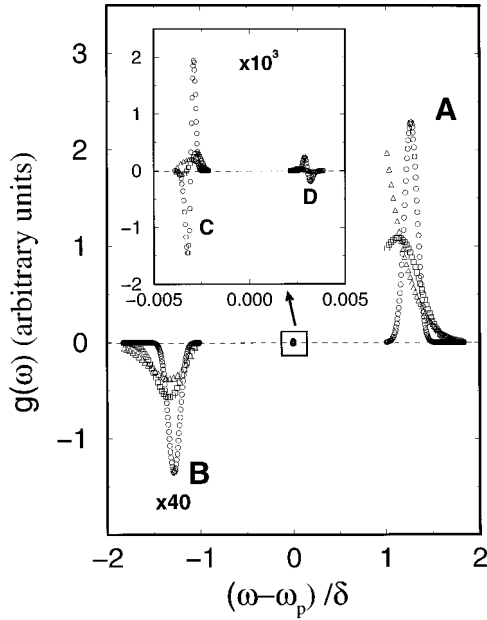


FIG. 4. Probe absorption for the photon statistics in Fig. 2 (single-atom case): triangles,  $r=0.98$ ; squares,  $r=1.03$ ; circles,  $r=1.5$ ; parameters:  $\delta=16g$ ,  $\langle\Omega\rangle=12.6g$ .

plitudes because of the nearly equal occupation probabilities of the states involved. They have no counterpart in the semiclassical approach.

The occupation probability  $p_n |\langle\mu_1, k=n|n; m=-1/2\rangle|^2$  of the dressed state  $|\mu_1, k=n\rangle$  depends, for sufficiently high detuning  $\delta$ , on the photon number  $n$  mainly by means of the photon number distribution  $p_n$ . Thus the absorbing transitions A reflect the shape of the photon statistics, as a comparison of Figs. 3 and 4 clearly shows.

### B. Absorption for two atoms

The probe absorption for two atoms for the Poisson-like photon statistics of a laser is shown in Fig. 5. A striking difference compared to the single-atom spectrum appears in groups A and B, which each consists of two subgroups of resonances with different amplitudes. In the inset of Fig. 5

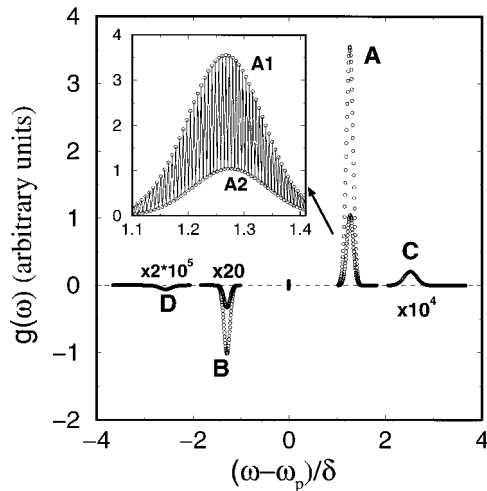


FIG. 5. Probe absorption for two atoms; parameters as in Fig. 4; photon statistics: laser above threshold ( $r=1.5$ ).

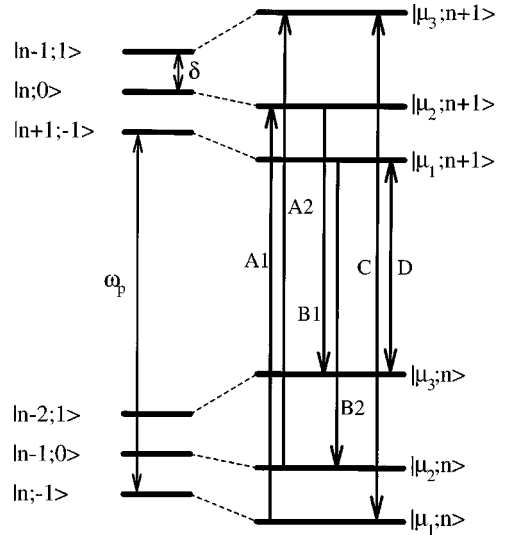


FIG. 6. Bare states and dressed states for the two-atom case.

the two subgroups of A are labeled by A1 and A2. A strong variation of the probe absorption results when changing the probe frequency slightly. Moreover, there are two groups of resonances C and D which have no counterpart in the single-atom case and the semiclassical case. Three further groups of resonances also appear in the central region  $\omega \approx \omega_p$ , which are not resolved in Fig. 5.

The new features can be interpreted along lines similar to those in Sec. IIIA. In the two-atom case, the finite subset of bare states mixed by the atom-photon interaction is

$$\{|n-2; m=+1\rangle, |n-1; m=0\rangle, |n; m=-1\rangle\}. \quad (3.4)$$

Two of these bare state triplets are shown on the left-hand side of Fig. 6. The corresponding dressed states shown on the right-hand side are shifted relative to the bare states, and again these shifts depend on the excitation number. The transitions are labeled according to Fig. 5.

For a sufficiently high detuning  $\delta$  of the order of  $\langle\Omega\rangle$ , the occupation probabilities  $|\langle\mu_i, n|n; m=-1\rangle|^2$ ; ( $i=1,2,3$ ) of the dressed states obey the relation

$$|\langle\mu_1, n|n; m=-1\rangle|^2 \gg |\langle\mu_2, n|n; m=-1\rangle|^2 > |\langle\mu_3, n|n; m=-1\rangle|^2. \quad (3.5)$$

In this case, transition A1 leads to a considerably stronger absorption than transition A2, representing a resonance of subgroup A2, as seen in the inset of Fig. 5. Since the transition frequencies of A1 and A2 are slightly different, a large variation of the absorption amplitude results. The two subgroups of B in Fig. 5, represented by the transitions B1 and B2 in Fig. 6, are to be explained by analogous arguments. The groups of resonances C and D are small because of small transition matrix elements.

In Fig. 7, the absorption spectrum for a detuning  $\delta$  significantly smaller than the mean Rabi frequency  $\langle\Omega\rangle$  is shown. Here subgroup A1 causes a probe gain, and the subgroups of B behave similarly. This is due to a dramatic change of the population distribution within a triplet with decreasing detuning  $\delta$ , as shown in Fig. 8, for the two lower dressed states. For large  $\delta$  the occupation probability of

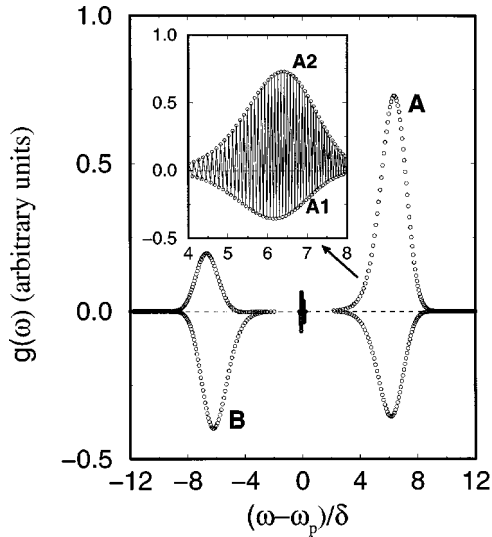


FIG. 7. Probe absorption for two atoms with nonclassical gain in  $A$  and absorption in  $B$ ; parameters:  $\delta=2g$ ,  $\langle\Omega\rangle=12.6g$ ; photon statistics: laser above threshold ( $r=1.5$ ).

$|\mu_1, n\rangle$  is larger than that of  $|\mu_2, n+1\rangle$ , and transition  $A1$  in Fig. 6 leads to an absorption. For low detuning  $\delta$ , the population difference between these two states is inverted, and transition  $A1$  causes a probe gain.

### C. Absorption for more than two atoms

If the number of atoms  $N_0$  is further increased, the absorption spectra become more and more complex. The number of subgroups increases as  $N_0$ , since  $N_0+1$  is the number of states within a dressed state multiplet, provided that the excitation number is not less than the number of atoms. An example for six atoms is shown in Fig. 9. Here the population inversion between the lowest dressed states within a multiplet appears even at a detuning  $\delta$  of the order of the mean Rabi frequency  $\langle\Omega\rangle$ . Thus one subgroup of  $A$  causes a probe gain.

As already mentioned in the introduction, it will be rather difficult to resolve the fine substructure in the lines because of homogeneous and inhomogeneous broadening. For example, the detection of the substructures for two atoms re-

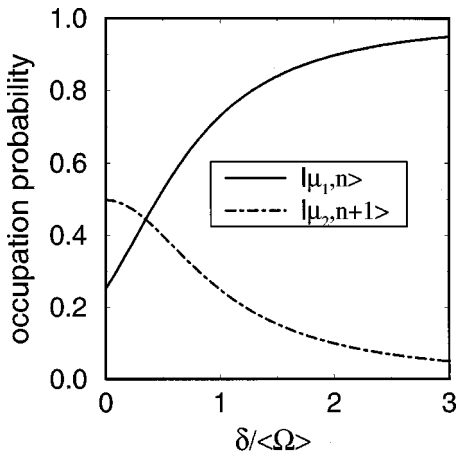


FIG. 8. Occupation probability of  $|\mu_1, n\rangle$  and  $|\mu_2, n+1\rangle$  vs pump detuning  $\delta$ ; parameters:  $\langle\Omega\rangle=20g$ ,  $n=\langle n\rangle=100$ .

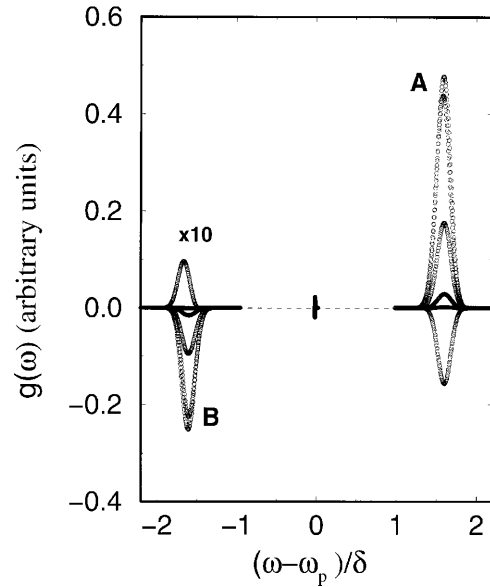


FIG. 9. Probe absorption for six atoms; parameters:  $\delta=16g$ ,  $\langle\Omega\rangle=20g$ ; photon statistics: laser above threshold ( $r=1.5$ ).

quires a line width less than  $0.1g$ . Nevertheless, the spectra with the unresolved substructure still reflect the pump photon statistics reasonably well, as shown in Fig. 10. Here we have assumed a homogeneous line broadening of  $0.4g$ .

In order to observe the photon statistics via the line shape of the Stark-shifted probe absorption, the line broadening should not exceed the coupling constant  $g$  drastically. If a pump-probe experiment in semiconductor physics is considered, narrow resonances of impurity-bound excitons can have a linewidth as low as  $40\ \mu\text{eV}$  [26]. Using common dipole matrix elements, we have estimated a coupling con-

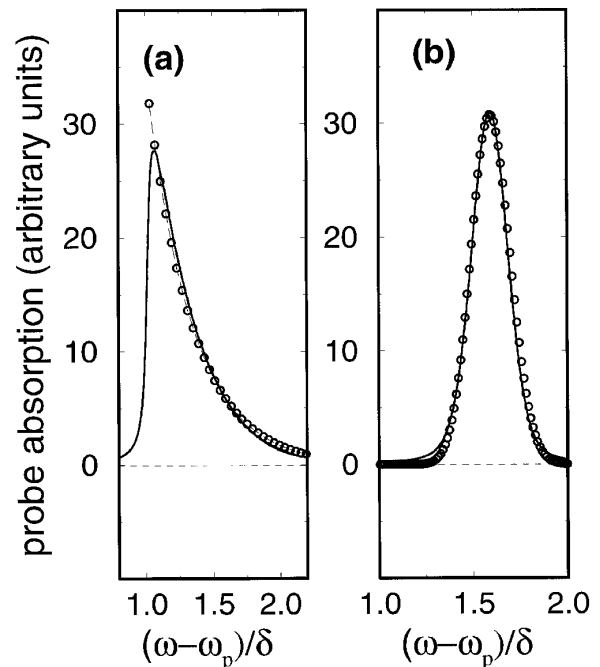


FIG. 10. Probe absorption ( $A$  transition) for six atoms with assumed spectral broadening for thermal-like (a) and Poisson-like (b) photon statistics; the statistics' shapes are also included (circles); parameters as in Fig. 9.

stant  $g$  of the order of  $10 \mu\text{eV}$ . Consequently, the influence of the photon statistics on the Stark-shifted absorption line shape might be observable for these narrow excitonic resonances, although possibly not as clear as in Fig. 10.

#### IV. SUMMARY

We have shown in this paper that the probe detection of resonances shifted by the optical Stark effect may provide a tool to measure the photon statistics of the pump. Moreover, we have found nonclassical features in multiatom spectra that have no counterpart in the single-atom case; i.e., high

variations of absorption amplitudes and nonclassical gain and absorption of the probe. The dressed state model gives an insight into the processes which cause these nonclassical features.

#### ACKNOWLEDGMENT

This work was supported by the Deutsche Forschungsgemeinschaft within the topical project ‘‘Quantum Coherence in Semiconductors.’’

- 
- [1] S. H. Autler and C. H. Townes, *Phys. Rev.* **100**, 703 (1955).
  - [2] F. Y. Wu, S. Ezekiel, M. Ducloy, and B. R. Mollow, *Phys. Rev. Lett.* **38**, 1073 (1977).
  - [3] Ph. Tamarat, B. Lounis, J. Bernard, M. Orrit, S. Kummer, R. Kettner, S. Mais, and Th. Basché, *Phys. Rev. Lett.* **75**, 1514 (1995).
  - [4] D. Fröhlich, A. Nöthe, and K. Reimann, *Phys. Rev. Lett.* **55**, 1335 (1985).
  - [5] A. Mysyrowicz, D. Hulin, A. Antonetti, A. Migus, W. T. Maselink, and H. Morkoc, *Phys. Rev. Lett.* **56**, 2748 (1986).
  - [6] S. Schmitt-Rink, D. S. Chemla, and H. Haug, *Phys. Rev. B* **37**, 941 (1988).
  - [7] R. Zimmermann, *Adv. Solid State Phys.* **30**, 295 (1990).
  - [8] E. T. Jaynes and F. W. Cummings, *Proc. IEEE* **51**, 89 (1963).
  - [9] B. W. Shore and P. L. Knight, *J. Mod. Opt.* **40**, 1195 (1993).
  - [10] R. Zimmermann and M. Hartmann, *Phys. Status Solidi B* **150**, 365 (1988).
  - [11] G. S. Agarval, *Phys. Rev. Lett.* **37**, 1383 (1976).
  - [12] H. J. Kimble and L. Mandel, *Phys. Rev. A* **15**, 689 (1977).
  - [13] G. Vemuri, K. V. Vasavada, and G. S. Agarval, *Phys. Rev. A* **50**, 2599 (1994).
  - [14] M. Brune, F. Schmidt-Kaler, A. Maali, J. Dreyer, E. Hagley, J. M. Raimond, and S. Haroche, *Phys. Rev. Lett.* **76**, 1800 (1996).
  - [15] N. Peyghambarian, S. W. Koch, M. Lindberg, B. Fluegel, and M. Joffre, *Phys. Rev. Lett.* **62**, 1185 (1989).
  - [16] M. Joffre, D. Hulin, A. Migus, and M. Combescot, *Phys. Rev. Lett.* **62**, 74 (1989).
  - [17] J. J. Bollinger, J. D. Prestage, W. M. Itano, and D. J. Wineland, *Phys. Rev. Lett.* **54**, 1000 (1985).
  - [18] F. Diedrich, J. C. Bergquist, W. M. Itano, and D. J. Wineland, *Phys. Rev. Lett.* **62**, 403 (1989).
  - [19] B. Appasamy, I. Siemers, Y. Stalgies, J. Eschner, R. Blatt, W. Neuhauser, and P. E. Toschek, *Appl. Phys. B* **60**, 473 (1995).
  - [20] R. J. Cook and H. J. Kimble, *Phys. Rev. Lett.* **54**, 1023 (1985).
  - [21] M. Tavis and F. W. Cummings, *Phys. Rev.* **170**, 379 (1968).
  - [22] R. H. Dicke, *Phys. Rev.* **93**, 99 (1954).
  - [23] S. M. Dutra, P. L. Knight, and H. Moya-Cessa, *Phys. Rev. A* **49**, 1993 (1994).
  - [24] G. D. Mahan, *Many-Particle Physics* (Plenum, New York, 1990).
  - [25] R. Loudon, *The Quantum Theory of Light* (Clarendon, Oxford, 1973).
  - [26] B. Lummer, J. M. Wagner, R. Heitz, A. Hoffmann, I. Broser, and R. Zimmermann, *Phys. Rev. B* **54**, 16727 (1996).